AIAA 80-0037R

Direct Fourier Synthesis of Waves: Application to Acoustic Source Radiation

Sébastien M. Candel* and Come Crance†
Office National d'Etudes et de Recherches Aérospatiales, Châtillon, France

In numerous situations of current interest in aeroacoustics the sound field propagates in a nonhomogeneous medium. This is typically the case of jet noise radiation. A widely used model in that situation consists of a thin vortex sheet separating two uniformly moving fluids. This model may be treated as a layered medium, and acoustic source radiation may be analyzed by Fourier transform techniques. The inversion of the Fourier solution is however difficult and requires far-field approximations. This difficulty is here avoided by constructing the wave field by direct Fourier synthesis. This method was shown, in a previous work to be fast, reliable, and superior to the standard approximations. It is applied here to source radiation in the vicinity of a vortex sheet separating uniformly moving streams. Complete wave field maps are given for subsonic and supersonic flow combinations, providing new insights on jet noise radiation and refraction in open wind tunnels.

Nomenclature

c = sound speed
C = characteristic lines
G = line source field in free space
J_0 = Bessel function of order zero
H_0^1 = Hankel function of order zero satisfying the radiation condition at infinity
h = source-interface distance
i = complex number, $\sqrt{-1}$
k = wave number
L = spatial extension of the calculation domain
M = Mach number
N = number of points used in the discrete Fourier transform
p = pressure
$\tilde{p}$ = Fourier transform of pressure
U = mean-flow velocity
x,z = Cartesian coordinates
α = spatial frequency, argument of Fourier transform
$\alpha_{j\pm}$ = branch points of $\gamma_j (j=1,2)$
γ_j = defined in text by Eq. (10)
$\delta(\ )$ = delta function
δ_j = defined in text by Eq. (11)
Δx = spatial sampling period
$\Delta\alpha$ = elementary spatial frequency filter
η = interfacial displacement
Θ = polar angle measured with respect to the x axis
λ = wavelength
ω = angular frequency

Subscripts

$*$ = reduced (dimensionless) quantity
j = subscript used to distinguish variables pertaining to region 1 ($z<0$) and region 2 ($z>0$)

I. Introduction

IN a recent Note[1] we showed that it is possible to solve a large number of wave propagation problems in stratified media by direct Fourier synthesis (DFS). With this technique it is possible to avoid the difficult or approximate computations of the standard analytical methods. In addition the solution obtained is exact except for errors associated with spectral aliasing. The power and efficiency of the DFS was clearly demonstrated in Ref. 1. We shall here apply this method to one of the fundamental problems encountered in aeroacoustics, that of sound source radiation in the vicinity of flow discontinuity. We specifically consider three configurations (Fig. 1). In the first case the source is embedded in a uniform flow of Mach number M_1 and radiates toward a medium at rest (Fig. 1a). This configuration may be used to model noise radiation from a fixed point in a freejet toward the ambient atmosphere (Fig. 1b). The second case (Fig. 1c) is that of a sound source radiating from a medium at rest toward a uniform flow. This situation is not often encountered in practice but it was found to be useful, for example, in an experimental analysis[2] of refraction effects in an open wind tunnel (Fig. 1d). The third case (Fig. 1e) is that where the source is in a uniform flow of Mach number $M_1>0$ and radiates toward a second medium flowing in the negative direction with a Mach number $-M_2<0$. This last case may be used as a schematic model of convective effects arising when a sound source moving at a Mach number M_2 radiates from a freejet of Mach number M_1+M_2 toward an ambient atmosphere at rest (Fig. 1f).

One interesting feature of the DFS is that it may be applied, with some precautions, to situations where the flow is supersonic. We shall see that the specific properties of such flows, such as the appearance of characteristic lines, discontinuity of the wavefield across the characteristic lines, and modification of the far field radiation condition, are correctly retrieved by direct Fourier synthesis of the wavefield.

It is now worth reviewing some of the numerous studies dealing with the problems we have just defined. The first analysis of the configurations sketched on Figs. 1a and c seems to be due to Gottlieb.[3] The solution was obtained by applying a Fourier transformation in the direction parallel to the flow and then using the method of stationary phase to invert the final Fourier integral. This last operation was performed by first writing the phase appearing in the integral in terms of polar coordinates. The polar coordinates' origin was taken to be the point of the interface situated upright from the source. Now we show in Ref. 1 that this choice essentially determines the quality of the stationary phase approximation. Indeed, the straightforward choice made by Gottlieb (and by many authors) leads to results that are not quite satisfactory: a region is formed where the field amplitude decays exponentially, the wavefield is discontinuous

Presented as Paper 80-0037 at the AIAA 18th Aerospace Sciences Meeting, Pasadena, Calif., Jan 14-16, 1980; submitted Jan. 16, 1980; revision received Sept. 23, 1980.

*Research Scientist, also Professor of Engineering, Ecole Centrale des Arts et Manufactures. Member AIAA.

†Research Scientist, now at Service Technique des Constructions et Armes Navales.

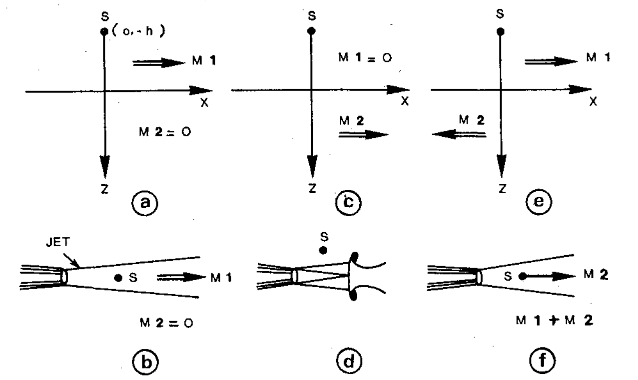

Fig. 1 Geometries of the problems treated and corresponding real configurations.

on the boundary of this region, and the wavefronts exhibit an inverted curvature near that boundary. The most visible consequence is that the radiation diagrams computed have cusps and abrupt discontinuities. These difficulties may be avoided by a suitable choice of the polar coordinate origin (see Ref. 1).

In a more recent study of great elegance, Ffowcs Williams[4] considers noise production at the edge of a steady flow. The radiation patterns obtained are similar to those of Gottlieb, and Ffowcs Williams notes that the sound field is determined in an essential way by the discontinuous structure of the flowfield. The radiation diagrams here too have cusps, and one notes that for supersonic flow velocities acoustic radiation is very nearly omnidirectional except for a reduced region of silence situated downstream. The calculated sound distribution is compared to the observed sound field of a helium jet exhausting from a nozzle at a Mach number $M_1 = 4.3$ and only limited agreement is reached. In the Schlieren image of the sound field, radiation in the upstream region is not important and the region of silence predicted is not observed.

Another interesting study of radiation problems in the presence of velocity discontinuity is that of Howe.[5] His analysis is based on the principle of conservation of energy but a far-field approximation is also needed. The results obtained while of greater generality do not differ from those found by application of the method of stationary phase.

A very pertinent study is that of Mani.[6] This author considers in great detail the influence of flow on noise radiation from a jet. The problem is treated in cylindrical geometry and a Fourier transform is first performed in the axial direction. The method of stationary phase is used in the final step and yields analytical expressions for the far field. For an angle of observation Θ such that $0 \leq \Theta \leq \cos^{-1}(1/1+M_1)$ the sound field amplitude decreases exponentially. The decay rate increases with frequency, and as a consequence discrepancies arise between theory and experiment at Strouhal numbers greater than or equal to one (for example, Figs. 7d and 10d of Ref. 6).

The previous studies consider essentially monochromatic source radiation. Transient problems are analyzed in particular by Friedland and Pierce,[7] Howe,[8] Jones,[9] and Chao.[10] These authors are mainly concerned with the instability wave that arises in the transient problem. An interesting technique is used by Chao[10] to invert the space-time Fourier transform. The technique is an extension of Cagniard's method but the computation of the transmitted wave still requires the method of stationary phase.

In most of the studies cited one finds the same difficulties arising from the classical application of far-field approximations. These difficulties are avoided when the wavefield is computed by direct Fourier synthesis.[1]

For simplicity we consider a two-dimensional geometry like Gottlieb,[2] Ffowcs Williams,[4] and Howe[5] but note that the cylindrical problem formulated by Mani[6] may be solved with no difficulty by DFS. For completeness a mathematical analysis of the problem is given in Sec. II. Section III gives some practical details on the DFS, and Sec. IV presents results for subsonic configurations. Section V deals with acoustic radiation of a source placed in a uniform supersonic stream. This classical problem is treated to demonstrate that the DFS may be used in a situation where the propagation equation is hyperbolic. Supersonic configurations are then examined in Sec. VI.

II. Formulation of the Problem

The formulation of the problem is similar to that given by Gottlieb. We consider a line source of amplitude 4π placed at $z = -h$ in a uniform stream (region 1) of Mach number M_1, sound speed c_1, and density ρ_1. The plane $z = 0$ separates region 1 ($z < 0$) from region 2 ($z > 0$) where the Mach number is M_2, the sound speed c_2, and the density ρ_2. We only consider monochromatic waves having a common factor $\exp(-i\omega t)$.

The wavefield is then the solution of convected wave equations in the two half spaces:

$$(1-M_1^2)p_{xx} + p_{zz} + 2ik_1M_1p_x + k_1^2p = -4\pi\delta(z+h)\delta(x), \qquad z<0 \tag{1}$$

$$(1-M_2^2)p_{xx} + p_{zz} + 2ik_2M_2p_x + k_2^2p = 0, \qquad z>0 \tag{2}$$

where $k_1 = \omega/c_1$ and $k_2 = \omega/c_2$.

Matching conditions at the $z = 0$ plane are obtained by specifying that pressure and normal displacement η are continuous across the interface

$$p(x,0_+) = p(x,0_-), \qquad \eta(x,0_+) = \eta(x,0_-) \tag{3}$$

where the normal displacement is obtained from the linearized momentum equations

$$\left(-i\omega + U_1\frac{\partial}{\partial x}\right)^2 \eta(x,0_-) = -\frac{1}{\rho_1}\frac{\partial p}{\partial z}(x,0_-) \tag{4}$$

$$\left(-i\omega + U_2\frac{\partial}{\partial x}\right)^2 \eta(x,0_+) = -\frac{1}{\rho_2}\frac{\partial p}{\partial x}(x,0_+) \tag{5}$$

The wavefield must also satisfy a radiation condition at infinity. If the motion is subsonic, this condition is similar to that given by Sommerfeld for a medium at rest (see, for instance, Ref. 11). In a supersonic stream a different condition applies.[11,12]

The previous problem may be solved by Fourier methods. We define the transforms $\tilde{p}_1(\alpha,z)$, $\tilde{p}_2(\alpha,z)$ of the field in regions 1 and 2 by

$$p(x,z) = \int \tilde{p}_j(\alpha,z)e^{i\alpha x}\mathrm{d}\alpha \qquad \text{for } j=1,2 \tag{6}$$

The transformed problem then is written

$$\frac{\mathrm{d}^2\tilde{p}_j}{\mathrm{d}z^2} - \gamma_j^2\tilde{p} = -2\delta(z+h) \qquad \text{for } j=1,2 \tag{7}$$

$$\tilde{p}_1(\alpha,0_-) = \tilde{p}_2(\alpha,0^+) \tag{8}$$

$$\frac{1}{\rho_1c_1^2\delta_1^2}\frac{\mathrm{d}\tilde{p}_1}{\mathrm{d}z}(\alpha,0_-) = \frac{1}{\rho_2c_2^2\delta_2^2}\frac{\mathrm{d}\tilde{p}_2}{\mathrm{d}z}(\alpha,0_+) = \tilde{\eta}(\alpha) \tag{9}$$

where

$$\gamma_j = [(1-M_j^2)\alpha^2 + 2M_jk_j\alpha - k_j^2]^{1/2}, \qquad j=1,2 \tag{10}$$

and

$$\delta_j = k_j - M_j \alpha, \qquad j = 1,2 \tag{11}$$

γ_1 and γ_2 each have two branch points situated at

$$\alpha_{j+} = \frac{k_j}{1+M_j} \text{ and } \alpha_{j-} = -\frac{k_j}{1-M_j}, \qquad j=1,2 \tag{12}$$

It is necessary, therefore, to select a proper determination of γ_1 and γ_2. The choice must be consistent with the radiation condition at infinity and it may be guided by assuming that α is complex, and by considering the integration path of the Fourier transforms in the complex plane. It is also convenient to assign to wave numbers k_j a small positive imaginary part k_{ij}. The branch points leave the real axis, a branch cut may be defined in the complex plane (Fig. 2), and the determination of γ_j is obtained by making use of arguments similar to those given by Noble.[13] For a subsonic stream the branch points are in the first and third quadrant, the integration path is parallel to the real axis, and it must be drawn between these two points (Fig. 2a). Letting k_{ij} tend to zero one obtains Fig. 2b, and one determination of γ_j in accord with Fig. 2b is

$$\gamma_j = (1-M_j^2)^{1/2} \,|\, (\alpha-\alpha_{j+})(\alpha-\alpha_{j-}) \,|^{1/2},$$
$$\alpha < \alpha_{j-} \text{ or } \alpha > \alpha_{j+}$$

$$\gamma_j = i(1-M_j^2)^{1/2} \,|\, (\alpha-\alpha_{j+})(\alpha-\alpha_{j-}) \,|^{1/2},$$
$$\alpha_{j-} \leq \alpha \leq \alpha_{j+} \tag{13}$$

For a supersonic stream both branch points are in the first quadrant and the integration path is placed above these points (Fig. 2c). A consistent determination of γ_j is now

$$\gamma_j = (M_j^2-1)^{1/2} \,|\, (\alpha-\alpha_{j+})(\alpha-\alpha_{j-}) \,|^{1/2}, \quad \alpha_{j+} \leq \alpha \leq \alpha_{j-}$$
$$\gamma_j = i(M_j^2-1)^{1/2} \,|\, (\alpha-\alpha_{j+})(\alpha-\alpha_{j-}) \,|^{1/2}, \quad \alpha_{j-} < \alpha$$
$$\gamma_j = -i(M_j^2-1)^{1/2} \,|\, (\alpha-\alpha_{j+})(\alpha-\alpha_{j-}) \,|^{1/2}, \quad \alpha < \alpha_{j+} \tag{14}$$

Straightforward calculations then yield the solution of the transformed problem Eqs. (7-9) and an integral expression of

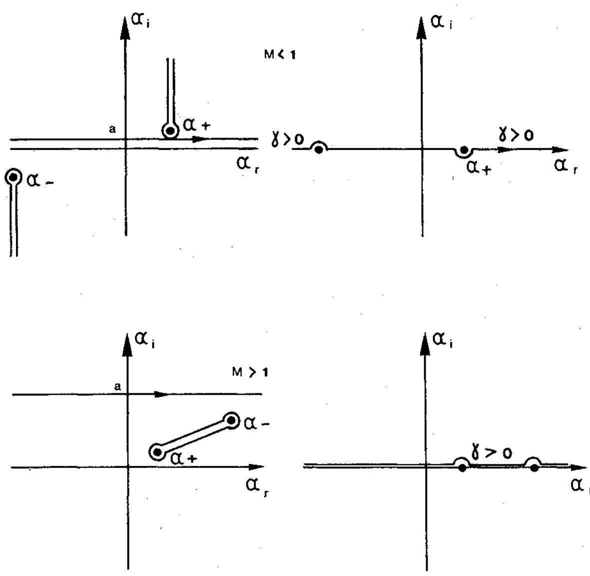

Fig. 2 Integration path in the complex α plane and associated branch cuts; a) and b) subsonic flow, c) and d) supersonic flow.

the pressure field is thus obtained

$$p(x,z) = \int \frac{\exp[-\gamma_1 \,|\, z+h \,|\, + i\alpha x]}{\gamma_1} \mathrm{d}\alpha$$
$$- \int \frac{\exp[\gamma_1 (z-h) + i\alpha x]}{\gamma_1} \mathrm{d}\alpha + \int \exp[\gamma_1 (z-h) + i\alpha x]$$
$$\times \frac{2\rho_2 c_2^2 \delta_2^2}{\rho_1 c_1^2 \delta_1^2 \gamma_2 + \rho_2 c_2^2 \delta_2^2 \gamma_1} \mathrm{d}\alpha, \qquad z \leq 0 \tag{15}$$

$$p(x,z) = \int \exp[-\gamma_1 h - \gamma_2 z + i\alpha x]$$
$$\times \frac{2\rho_2 c_2^2 \delta_2^2}{\rho_1 c_1^2 \delta_1^2 \gamma_2 + \rho_2 c_2^2 \delta_2^2 \gamma_2} \mathrm{d}\alpha, \qquad z \geq 0 \tag{16}$$

The first two terms appearing in the expression Eq. (15) are identified as the direct wave G_{1+} emitted by the source and a reflected wave G_{1-} of same amplitude emitted in antiphase by the source image. The two waves are convected at a Mach number M_1. In a subsonic situation ($M_1 < 1$) these waves are cylindrical and given by

$$G_{1\pm} = \frac{\pm i\pi}{(1-M_1^2)^{1/2}} \exp \frac{-ik_1 M_1 x}{1-M_1^2}$$
$$\times H_0^1 \left\{ \frac{k_1}{1-M_1^2} [x^2 + (z \pm h)^2 (1-M_1^2)]^{1/2} \right\} \tag{17}$$

The form and character of these waves changes notably if the stream is supersonic ($M_1 > 1$). It may be shown that

$$G_{1\pm} = \frac{\pm 2\pi}{(M_1^2-1)^{1/2}} \exp \frac{ik_1 M_1 x}{M_1^2 - 1}$$
$$\times J_0 \left\{ \frac{k_1}{M_1^2-1} [x^2 - (z \pm h)^2 (M_1^2-1)]^{1/2} \right\}$$
$$\text{if } x^2 \leq (M_1^2-1)(z \pm h)^2 \text{ and } x \geq 0$$
$$= 0 \quad \text{if } x^2 \leq (M_1^2-1)(z \pm h)^2 \text{ or } x \leq 0 \tag{18}$$

The sound field G_{1+} vanishes identically upstream of the characteristic lines $x = \pm (M_1^2-1)^{1/2}(z+h)$ issuing from the source and a similar phenomenon is observed for the reflected wave G_{1-}. We shall see in Sec. V that this behavior is retrieved correctly by direct Fourier synthesis. The third term of expression Eq. (15) and the only term of expression Eq. (16) do not allow a simple evaluation. However, these two terms are Fourier transforms and their synthesis may be performed by making use of the fast Fourier transform algorithm (FFT).

III. Direct-Fourier Synthesis: Practical Aspects

Following Ref. 1 we introduce a set of reduced variables $x_* = x/L$, $z_* = z/L$, $h_* = h/L$ where L designates the spatial extension of the calculation domain ("the spatial window"). It is then natural to define the following set of reduced wave numbers $k_{1*} = k_1 L$, $k_{2*} = k_2 L$, $\alpha_* = \alpha L$. Expressions Eqs. (15) and (16) are not modified by this change of variables and the asterisk may be suppressed. Now, evaluation of Eqs. (15) and (16) is to be conducted with an N point FFT.

The spatial sampling period is then $\Delta x = 1/N$, the elementary spatial filter $\Delta\alpha = 2\pi$, and the maximum spatial frequency is, therefore, $\alpha_{max} = (N/2)2\pi$. Application of the FFT algorithm induces various distortions, the main source of error being spectral aliasing associated with the finite spatial

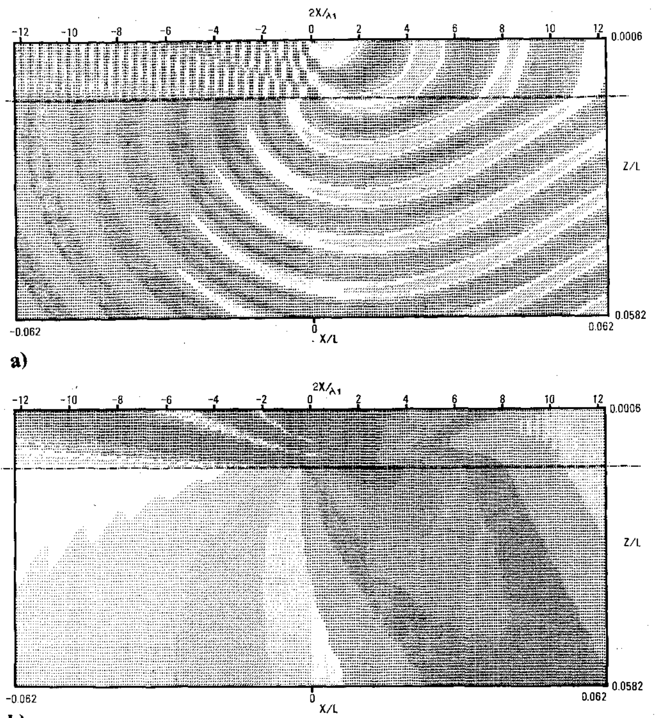

Fig. 3 Source radiation in configuration Fig. 1a: $M_1 = 0.8$, $M_2 = 0$; reduced wavenumbers, $k_1L = k_2L = 100.5(2\pi)$, $h/L = 0.016$. A ten level gray scale is used in all figures. a) Real part of the field, the gray levels represent the $(-1, +1)$ interval, and b) modulus of the field, the gray levels represent the (0,1) interval.

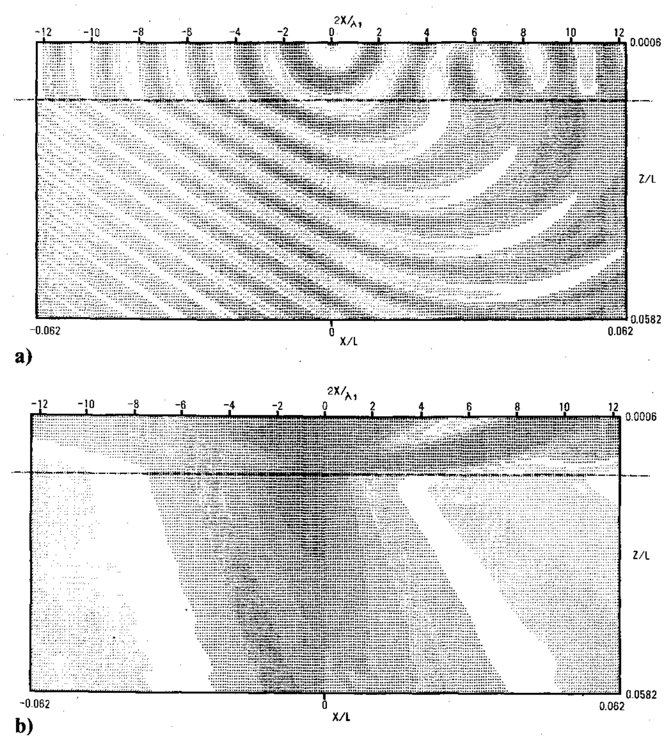

Fig. 4 Source radiation in configuration Fig. 1b: $M_1 = 0$, $M_2 = 0.8$; $k_1L = k_2L = 100.5(2\pi)$; $h/L = 0.016$. a) Real part of the wavefield; b) modulus. Gray scales are similar to those of Fig. 3.

frequency bandwidth.[1] It is also important to recall that the Fourier transforms on the real axis must be interpreted as Cauchy principal values in the vicinity of the branch points. In discrete form this rule may be obeyed by placing the branch points α_+ and α_- at the centers of sampling intervals. Now, if k and M have given values at the outset, a slight change in one parameter is required (for instance, if $k = 100.5\ \Delta\alpha$ and $M = 0.8$ the branch points may be placed at $\alpha_+ = 55.5\ \Delta\alpha$ and the new value of k is $99.96\ \Delta\alpha$).

IV. Source Radiation in Subsonic Situations

All the results presented have been obtained with a 2048 point Fourier transform. Only 256 points surrounding the source are generally displayed. In all calculations the sound speeds in regions 1 and 2 are identical and the reduced spatial wave numbers are $k_1L = k_2L = 100.5\ \Delta\alpha$. The corresponding wavelength for a medium at rest is then such that $\lambda/L = 1/100.5$ so that the calculation domain extends over 100.5 wavelengths.

The first calculation (Figs. 3a and b) corresponds to the configuration sketched on Fig. 1a. The source is in a medium flowing at a Mach number $M_1 = 0.8$ and radiates toward a medium at rest ($M_2 = 0$). The source-interface distance is $h/L = 34\Delta x = 0.016$. The wavefronts emitted by the source are convected in the positive x direction and form a family of conjugate circles (Fig. 3a). The reflected wave amplitude is more important upstream and a characteristic interference pattern results from its combination with the direct wave (Fig. 3a). In the downstream direction the reflected wave is weak and the direct wave dominates. In region 2 the transmitted wave fronts are ovalized. Their shape allows the fronts to propagate along the interfacial surface $z = 0$ with the phase velocity imposed in region 1. As a consequence, in the downstream region where the reflected wave is weak, the wavefronts are "phase locked" and the transition across the interface is smooth. Figure 3b displays the wavefield modulus. Upstream and in region 1 the direct and reflected waves interfere strongly and fringes are observed. In region 2 the transmittted wave has its maximum near the direction $\cos^{-1}(1/1 + M_1) = 56$ deg. The transmitted field amplitude changes smoothly, it diminishes in the rear arc near the interface, and a stronger reduction is observed in the forward arc. The results obtained here may be compared to calculations based on the geometrical approximation[14,15] concerning axial sources in free jets. The wavefront shapes are similar to those displayed on Fig. 3a. Radiation diagrams obtained in Ref. 14 are also in qualitative agreement with the structure of the transmitted wavefield of Fig. 3b.

The second configuration is of the type sketched on Fig. 1c. The source is in a medium at rest ($M_1 = 0$) and radiates toward a moving stream ($M_2 = 0.8$). Upstream and in region 1 the direct wave dominates a weak reflected wave (Fig. 4a). Downstream in the same medium the reflected wave amplitude is more important, especially for incidence angles $0 \le \Theta \le \cos^{-1}(1/1 + M_2)$, and an interference pattern is formed. Upstream and in medium 2 the wavefronts appear to be nearly parallel. This may be explained by resorting to a geometrical argument: near the interface the wavevector direction in region 2 is such that $\cos\Theta_2 = \cos\Theta_1/(1 - M_2\cos\Theta_1)$ and, as a consequence, for incident wavevector directions $130 \le \Theta_1 \le 180$ deg, angle Θ_2 belongs to a reduced interval $115 \le \Theta_2 \le 123$ deg. Then the wavefronts are nearly plane and form an angle of 25-33 deg with the interface (Fig. 4a). In the same medium but downstream and near the interface the wavevectors are essentially horizontal, and correspondingly the wavefronts intersect the interface at right angles. Looking now at Fig. 4b one notes that the contours of equal amplitude are "swept" downstream by the uniform flow in region 2. The field amplitude is reduced downstream near the $z = 0$ plane as a direct consequence of the strong reflection occurring in region 1.

The third configuration is that of Fig. 1e. The Mach numbers chosen are $M_1 = 0.32$ and $M_2 = -0.48$ corresponding to a situation where a source convects at $M_c = 0.48$ in a flow of Mach number $M_1 = 0.8$. The wavefield is observed in the reference frame of the source. In medium 1 the direct wave is convected by the flow in the positive direction. This wave is predominant downstream and combines with a

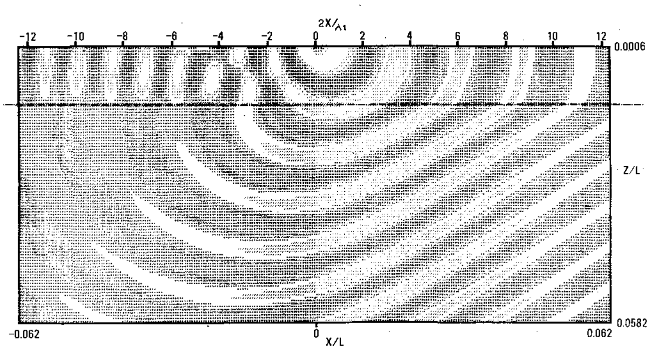

a)

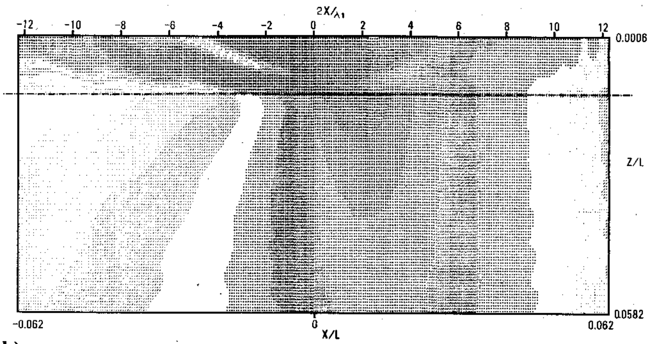

b)

Fig. 5 Source radiation in configuration Fig. 1e: $M_1 = 0.32$; $M_2 = -0.48$; $k_1L = k_2L = 100.5(2\pi)$; $h/L = 0.016$. a) Real part of the wavefield; b) modulus. Gray scales are similar to those of Fig. 3.

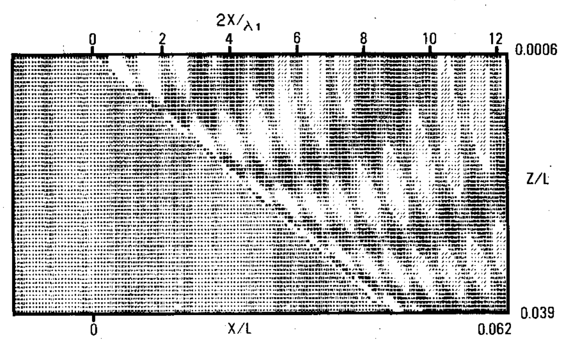

a)

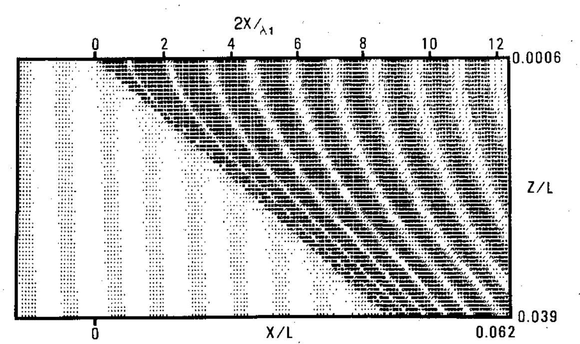

b)

Fig. 6 Source radiation in a uniform supersonic stream: $M_1 = 1.5$; $k_1L = 100.5(2\pi)$. a) Real part of the wavefield; b) modulus. Gray scales are similar to those of Fig. 3.

reflected wave upstream (Figs. 5a and b). In medium 2 the wavefronts are quasiplane upstream ($x \geq 0$) and nearly cylindrical downstream ($x \leq 0$). These features may be explained by a geometrical argument similar to that used for the second configuration. One also notes the formation of a directivity lobe near the z axis (Fig. 5b) and it is found that refraction in this configuration is more important than in the first case treated (Figs. 3a and b).

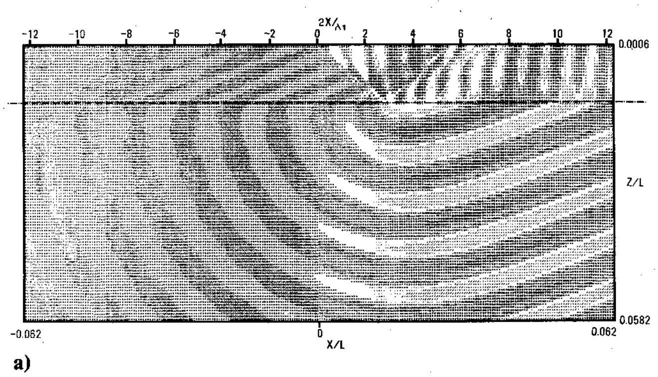

a)

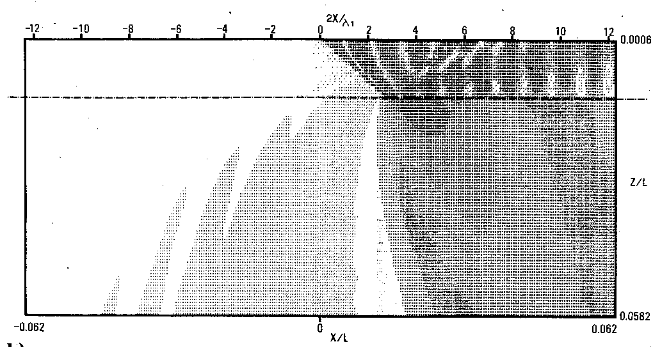

b)

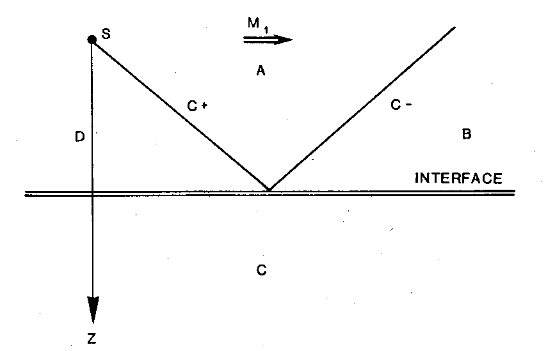

c)

Fig. 7 Source radiation in configuration Fig. 1a: medium 1 is supersonic, $M_1 = 1.5$, $M_2 = 0$; $k_1L = k_2L = 100.5(2\pi)$; $h/L = 0.016$. a) Real part of the wavefield; b) modulus; c) sketch of the field structure. Gray scales are similar to those of Fig. 3.

V. Source Radiation in a Uniform Supersonic Stream

Before dealing with situations involving a shear layer and supersonic streams it is worth showing that the DFS correctly retrieves the sound field of a source radiating in a uniform supersonic stream. In that situation the wavefield has the form Eq. (18) given in Sec. II. [Note: this field is of importance in unsteady potential flow theory and aeroelasticity (see, for example, Miles[12]).] Consider a source placed at the origin ($h = 0$), the sound field vanishes in the region situated upstream of the characteristic lines C_+ and C_- issuing from this point. Between C_+ and C_- the modulus varies like a Bessel function of zeroth order and the lines of constant amplitude are hyperbolas $x^2 - (M^2 - 1)z^2 = C$ asymptotic to C_+ and C_-. On the characteristics the field modulus is constant and equal to $2\pi/(M^2 - 1)^{1/2}$.

These features are indeed obtained by direct synthesis (Figs. 6a and b). The characteristic C_+ is well defined. At its left the field amplitude is weak and of the order of 0.1. The maximum amplitude is reached on C_+ and has the expected value $2\pi/(M^2 - 1)^{1/2} \simeq 5.6$. Now, as a consequence of spectral aliasing, the field amplitude does not vanish upstream. By increasing the size of the Fourier transform this error may be reduced. However, its relative magnitude (of about 1.5%) appears already suitable, and we kept $N = 2048$ to economize CPU time.

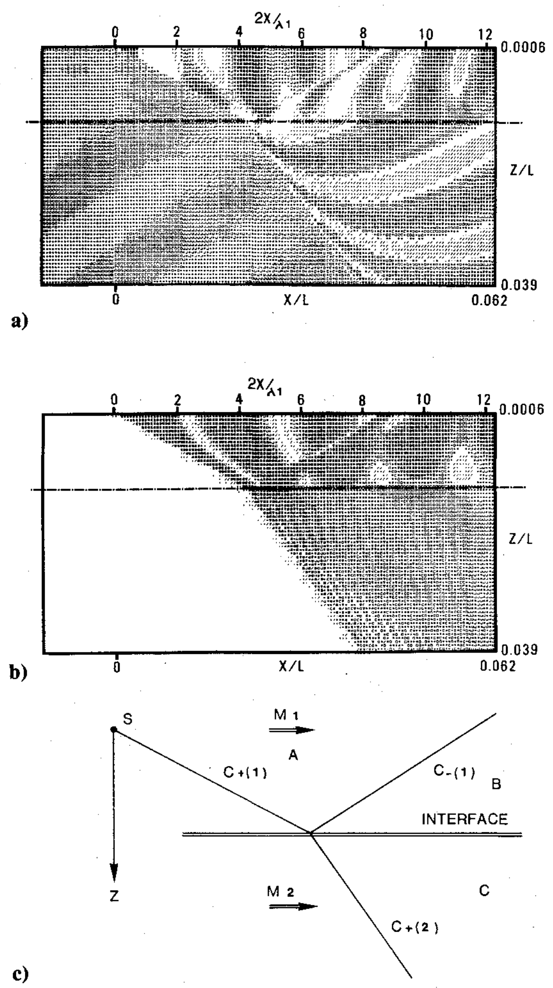

Fig. 8 Source radiation in configuration Fig. 1a: the two streams are supersonic, $M_1 = 2$, $M_2 = 1.2$; $k_1L = k_2L = 100.5(2\pi)$; $h/L = 0.016$. a) Real part of the wavefield; b) modulus; c) sketch of the field structure. Gray scales are similar to those of Fig. 3.

The structure of the real part of the wavefield deserves some additional comments. One distinguishes on Fig. 6a successive wavefronts emitted by the source and convected by the flow. Because the stream is supersonic these fronts are tangent to C_+, and fronts of equal phase intersect and form regions of higher amplitude while fronts of opposite phase create regions of vanishing amplitude. A characteristic interference fringe pattern results from this process.

VI. Source Radiation in the Presence of Supersonic Streams

We now consider, as a first example, a configuration of the type sketched on Fig. 1a with Mach numbers $M_1 = 1.5$ and $M_2 = 0$. Four different regions may be distinguished on Figs. 7a and b and the structure of the wavefield is sketched on Fig. 7c.

In region A, bounded by the characteristic C_+ originating at the source and the characteristic C_- reflected by the shear layer, the field is essentially formed by the direct wave radiated by the source in the supersonic stream. A diffracted wave resulting from the upstream propagation of the transmitted wave also arises in region A but its amplitude is small. As a consequence, the field structure in region A greatly resembles that described in Sec. V.

In region B, bounded by the reflected characteristic C_- and the shear layer, the direct wave combines with the wave reflected by the source image and an interference pattern is formed.

In region C (medium 2) the wavefronts appear strongly distorted (Fig. 7a). Quasiplane downstream, they become nearly cylindrical upstream, and their shape may be explained by geometrical arguments similar to those used in Sec. IV. The field reaches its maximum at an angle of about $\cos^{-1}(1/1+M_1) \simeq 66$ deg with the interface. Its amplitude is very weak upstream and, as a consequence, the diffracted wave that arises in region D (above the interface and upstream of C_+) is also weak.

Finally let us consider the same configuration but in the case where both streams are supersonic $M_1 = 2$, $M_2 = 1.2$ (Figs. 8a, b, and c). Three main regions are now apparent. In region A, bounded by the characteristic $C_+(1)$ and the reflected characteristic $C_-(1)$, only the direct wave propagates and the field has the structure described in Sec. V. In region B, defined by the reflected characteristic $C_-(1)$ and the shear layer, the direct and reflected waves interfere producing fringes. A transmitted wave is formed in region C between the characteristic $C_+(2)$ and the shear layer. Upstream of $C_+(1)$ and $C_+(2)$ the field vanishes.

VII. Discussion

The problems treated in this paper clearly show that direct Fourier synthesis constitutes a suitable and powerful tool for analyzing source radiation in the presence of flow. Many other cases may be dealt with by the same technique. It is, for instance, possible to study with only little effort source radiation in multiple jets and "inverted" configurations. The results obtained in Sec. VI also may be useful to the description of sound radiation by an oscillating shock impinging on a shear discontinuity.

References

[1] Candel, S. M. and Crance, C., "Direct Fourier Synthesis of Waves in Layered Media and the Method of Stationary Phase," accepted for publication in the *Journal of Sound and Vibration,* Vol. 74, Feb. 1981.

[2] Candel, S. M., Guédel, A., and Julienne, A., "Radiation Refraction and Scattering of Acoustic Waves in a Free Shear Flow," AIAA Paper 76-544, July 1976.

[3] Gottlieb, P., "Sound Source near a Velocity Discontinuity," *Journal of the Acoustic Society of America,* Vol. 32, Sept. 1960, pp. 1117-1122.

[4] Ffowcs Williams, J. E., "Sound Production at the Edge of Steady Flow," *Journal of Fluid Mechanics,* Vol. 66, 1974, pp. 791-816.

[5] Howe, M. S., "Application of Energy Conservation to the Solution of Radiation Problems Involving Uniformly Convected Source Distributions," *Journal of Sound and Vibration,* Vol. 43, Nov. 1975, pp. 77-86.

[6] Mani, R., "The Influence of Jet Flow on Jet Noise - Part 1. The Noise of Unheated Jets," *Journal of Fluid Mechanics,* Vol. 73, April 1976, pp. 753-778.

[7] Friedland, A. B. and Pierce, A. D., "Reflection of Acoustic Pulses from Stable and Unstable Interfaces between Moving Fluids," *The Physics of Fluids,* Vol. 12, 1969, pp. 1148-1160.

[8] Howe, M. S., "Transmission of an Acoustic Pulse through a Plane Vortex Sheet," *Journal of Fluid Mechanics,* Vol. 43, Aug. 1970, pp. 353-367.

[9] Jones, D. S., "The Scattering of Sound by a Vortex Sheet," *Journal of the Institute of Mathematics and its Applications,* Vol. 15, Feb. 1975, pp. 33-57.

[10] Chao, C. C., "Transmitted Sound Field due to an Impulsive Line or Point Acoustic Source Through a Plane Vortex Sheet," AIAA Paper 77-1353, 1977.

[11] Candel, S. M., "Analytical Studies of Some Acoustic Problems of Jet Engines," Ph.D. Thesis, California Institute of Technology, 1972.

[12] Miles, J. W., *Potential Theory of Unsteady Supersonic Flow,* Cambridge University Press, 1959.

[13] Noble, B., *Methods Based on the Wiener-Hopf Technique,* Pergamon Press, 1958.

[14] Candel, S. M., "Etudes Théoriques et Expérimentales de la Propagation Acoustique en Milieu Inhomogene et en Mouvement," These de Doctorat es Sciences, University of Paris VI, 1977; also ONERA Publ. 1977-1.

[15] Candel, S. M., "Numerical Solution of Conservation Equations Arising in Linear Wave Theory. Application to Aeroacoustics," *Journal of Fluid Mechanics,* Vol. 83, Dec. 1977, pp. 465-493.